Measurements of event properties and multi-differential jet cross sections and impact of CMS measurements on Proton Structure and QCD parameters

Anterpreet Kaur⋆ for the CMS Collaboration
Panjab University, Chandigarh, India

Abstract. We present results on the measurements of characteristics of events with jets including jet-charge, investigations of shapes and jet mass distributions. The measurements are compared to theoretical predictions including those matched to parton shower and hadronization. Multi-differential jet cross sections are also presented over a wide range in transverse momenta from inclusive jets to multi-jet final states. These measurements have an impact on the determination of the strong coupling constant as well as on parton distribution functions (PDFs) and are helpful in the treatment of heavy flavours in QCD analyses. We also show angular correlations in multi-jet events at highest center-of-mass energies and compare the measurements to theoretical predictions including higher order parton radiation and coherence effects. Measurements of cross sections of jet and top-quark pair production are in particular sensitive to the gluon distribution in the proton, while the electroweak boson production - inclusive or associated with charm or beauty quarks - gives insight into the flavour separation of the proton sea and to the treatment of heavy quarks in PDF-related studies.

1 Introduction

Jets are narrow collimated cones of stable particles (mainly hadrons) produced by the hadronization of partons (quarks or gluons) in high-energy particle interactions. The strong interactions between the partons are described by the theory called Quantum Chromodynamics (QCD). In a hard scattering process, partons are produced with high-transverse momentum (p_T) and give rise to a parton shower (PS) by emission of additional gluons and production of quark-antiquark pairs. This phase can be described by perturbative QCD (pQCD) approximations. In the non-perturbative phase, the colored partons hadronize into colorless objects in the form of collimated sprays known as jets. Jets are measured in particle detectors and studied in order to determine the properties of the original quarks. The distribution of particles and energy within a jet can also reveal information about both the production mechanism and underlying physics.

CMS [1] is one of the two multipurpose experiments at the Large Hadron Collider (LHC) at CERN, designed to see a wide range of particles and phenomena produced in high-energy proton-proton (pp) collisions in the LHC. This paper presents several studies of jet production performed by CMS with data from proton-proton collisions taken at centre-of-mass energies ($\sqrt{s}$) of 8 and 13 TeV during Run 1 and 2 of the LHC respectively, from 2012 until 2016. The CMS detector covers a solid

---

⋆e-mail: anterpreet.kaur@cern.ch

angle of almost 4π and consists of precise tracking devices around the interaction point, surrounded by calorimeters and muon chambers. In the CMS experiment, all particles are reconstructed and identified using a particle-flow (PF) algorithm, which combines the information from the individual subdetectors [2]. The four-vectors of particle candidates, reconstructed by the above technique, are used as input to the anti-k_t jet clustering algorithm [3]. The clustering is performed within the FASTJET package [4] using four-momentum summation. A factorized jet calibration procedure with corrections for pile-up and jet energy scale are applied. The data is also corrected for detector effects using an unfolding procedure which allows direct comparisons with theory. Theoretical predictions are obtained from various Monte Carlo (MC) event generators. To compare with measurements, the parton-level calculations must be complemented with corrections for nonperturbative (NP) effects that involve the modeling of hadronization (HAD) and multiparton interactions (MPI).

2 QCD multijet production

Inclusive jet production (p + p → jet + X) is a key process to test predictions of perturbative QCD (pQCD) over a wide region in phase space. It probes the parton-parton interaction and is sensitive to the value of the strong coupling constant, α_S and also provides the important constraints on the description of the proton structure, expressed by the parton distribution functions (PDFs).

2.1 Inclusive jet production

The double-differential inclusive jet cross sections [5] has been measured using data collected at $\sqrt{s}$ = 8 TeV corresponding to an integrated luminosity of 19.7 fb^{-1}. The measurement is presented as a function of jet transverse momentum p_T and absolute rapidity $|y|$ and covers a large range in jet p_T from 74 GeV up to 2.5 TeV, in six rapidity bins up to $|y|$ = 3.0. The region of low jet p_T, in particular the range from 21 to 74 GeV, has also been studied up to $|y|$ = 4.7, using a dedicated low-pileup 5.6 pb^{-1} data sample. Perturbative QCD, supplemented by a small nonperturbative and electroweak corrections, describes the data over a wide range of jet p_T and y as shown in Figure 1 (left). Using the probed p_T range and six different rapidity bins, the high-p_T jet cross section measurements are used to extract the value of the strong coupling constant. The best fitted value is $\alpha_s(M_Z) = 0.1164^{+0.0060}_{-0.0043}$ using the CT10 NLO PDF set. The running of the strong coupling constant as a function of the energy scale Q, $\alpha_S(Q)$, measured for nine different values of energy scale between 86 GeV and 1.5 TeV, is in good agreement with previous experiments and extends the measurement to the highest values of the energy scale as shown in Fig. 3. This measurement also probes hadronic parton-parton interaction over a wide range of x and Q. The QCD analysis of these data together with HERA DIS measurements illustrates the potential of the high-p_T jet cross sections to provide important constraints on the gluon PDF in a new kinematic regime.

Similarly a measurement of the double-differential cross section as a function of jet p_T and absolute rapidity $|y|$ has been performed for two jet sizes R = 0.4 and 0.7 using data collected at $\sqrt{s}$ = 13 TeV [6]. Data samples corresponding to integrated luminosities of 71 pb^{-1} and 44 pb^{-1} are used for absolute rapidities $|y|$ < 3 and for the forward region 3.2 < $|y|$ < 4.7, respectively. The comparison between data and predictions at NLO in perturbative QCD including corrections for nonperturbative and electroweak effects are shown in Fig. 1 (right) and it is observed that jet cross sections for the larger jet size of R = 0.7 are accurately described, while for R = 0.4 theory overestimates the cross section by 5–10% almost globally. This measurement is a first indication that jet physics is as well understood at $\sqrt{s}$ = 13 TeV as at smaller centre-of-mass energies in the phase space accessible with the new data.
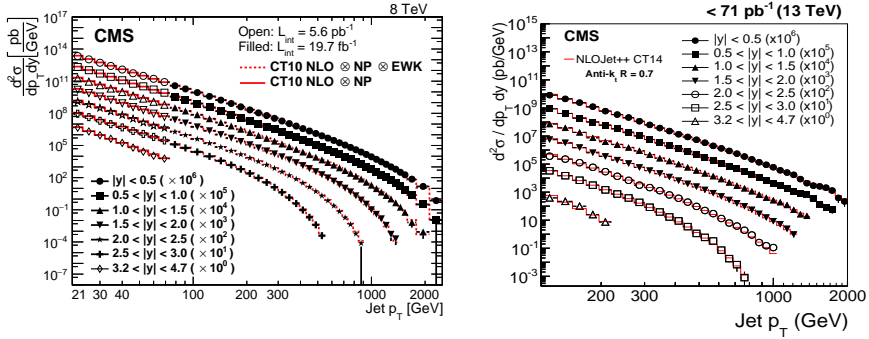
Figure 1. Double-differential inclusive jet cross sections as function of jet p_T for six different $|y|$ bins at an interval of $\Delta |y| = 0.5$. Left [5] : Data (open points representing the low-p_T analysis, filled points representing the high-p_T one) and NLO predictions based on the CT10 PDF set corrected for the nonperturbative factor for the low-p_T data (solid line) and the NP and electroweak correction factors for the high-p_T data (dashed line), at $\sqrt{s}$ = 8 TeV are shown. Right [6] : Data (points) and predictions from NLOJET++ based on the CT14 PDF set corrected for the NP and electroweak effects (line), at $\sqrt{s}$ = 13 TeV are shown.

2.2 Triple differential dijets

Measurements of dijet cross sections can be used to thoroughly test predictions of perturbative QCD (pQCD) at high energies and to constrain parton distribution functions (PDFs). A measurement of the triple-differential dijet cross section has been performed using CMS data collected at $\sqrt{s}$ = 8 TeV, as a function of the average transverse momentum $p_{T,avg} = \frac{1}{2}(p_{T,1} + p_{T,2})$ of the two leading jets, half of their rapidity separation $y^\star = \frac{1}{2}|y_1 - y_2|$, and the boost of the dijet system $y_b = \frac{1}{2}|y_1 + y_2|$ [7]. The data are found to be well described by NLO predictions corrected for nonperturbative and electroweak effects, except for highly boosted event topologies that suffer from large uncertainties in parton distribution functions (PDFs) as shown in Fig. 2 (left). For large values of y_b, the momentum fractions carried by the incoming partons must correspond to one large and one small value, while for small y_b the momentum fractions must be approximately equal. In addition, for high transverse momenta of the jets, x values are probed above 0.1, where the proton PDFs are less precisely known. From Fig. 2 (right), it is observed that the precise data constrain the PDFs, especially in the highly boosted regime that probes the highest fractions x of the proton momentum carried by a parton. Also in a simultaneous fit, the strong coupling constant $\alpha_s(M_Z)$ is extracted together with the PDFs and the value obtained at the mass of the Z boson is $\alpha_s(M_Z) = 0.1199 \pm 0.0015$ (exp)$^{+0.0031}_{-0.0020}$ (theo).

2.3 Inclusive multijets

The investigation of inclusive multijet event cross sections ($\sigma_{jet} \propto \alpha_S$) as a function of jet p_T and rapidity y provides essential information about the PDFs and the strong coupling constant. Moreover, the ratios of such cross sections, $R_{mn} = \frac{\sigma_{m-jet}}{\sigma_{n-jet}} \propto \alpha^{m-n}$, with m > n, provide an ideal tool to determine the strong coupling constant $\alpha_s(M_Z)$ as numerous theoretical and experimental uncertainties cancel. The inclusive 2- and 3-jet event cross sections as well as cross section ratio (R_{32}) have been measured using data corresponding to an integrated luminosity of 19.7 fb^{-1} at $\sqrt{s}$ = 8 TeV, as a function of the average transverse momentum, $H_{T,2}/2 = \frac{1}{2}(p_{T,1} + p_{T,2})$ of the two leading jets [9]. R_{32} as a function of $H_{T,2}/2$ is extracted from the data by dividing the differential cross sections for each bin in $H_{T,2}/2$.
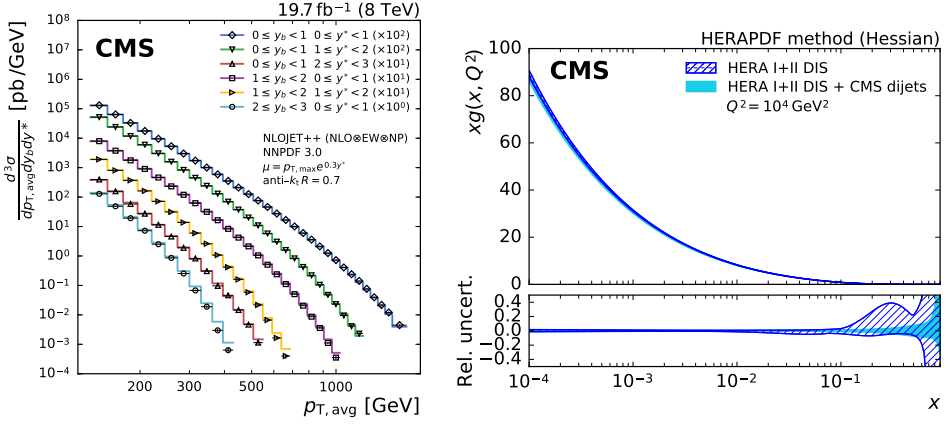
Figure 2. [7] Left : The triple-differential dijet cross section in six bins of $y^\star$ and y_b. The data are indicated by different markers for each bin. The theoretical predictions, obtained with NLOJET++ and NNPDF 3.0, and complemented with EW and NP corrections, are depicted by solid lines. Apart from the boosted region, the data are well described by the predictions at NLO accuracy over many orders of magnitude. Right : The gluon PDFs as a function of x as derived from HERA inclusive DIS data alone (hatched band) [8] and in combination with CMS dijet data (solid band). The PDFs are shown at the scale $Q^2 = 10^4 \, GeV^2$ with their total uncertainties.

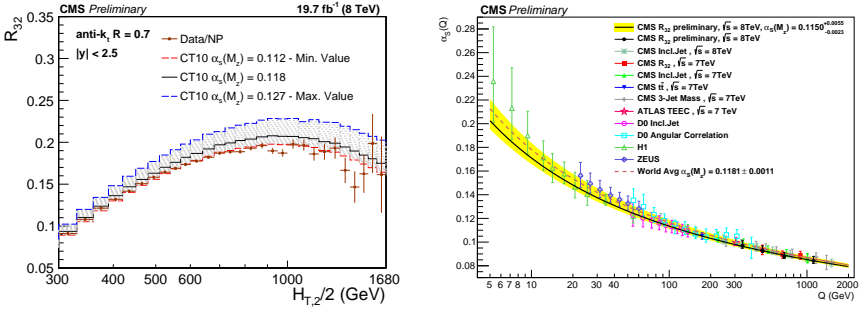**Figure 3.** [9] Left : Cross section ratio R_{32} as a function of $H_{T,2}/2$ calculated from data (solid circles) in comparison to that from NLO pQCD (lines). The NLO predictions using the CT10 NLO PDF set corrected with NP corrections are shown for a series of values assumed for $\alpha_s(M_Z)$ (dashed lines) together with the central prediction (solid line). Right : The running $\alpha_S(Q)$ as a function of the scale Q is shown. The dashed line represents the evolution of the world average [10] along with the results from other measurements of CMS [5, 11–14], ATLAS [15], D0 [16, 17], H1 [18, 19], and ZEUS [20].

Fig. 3 (left) presents this ratio as obtained from unfolded data in comparison to that from NLO pQCD using CT10 NLO PDF set corrected with NP corrections. From a fit of the ratio of the 3-jet over 2-jet event cross section using the MSTW2008 PDF set, the extracted value of strong coupling constant at the scale of the Z boson mass is $\alpha_s(M_Z) = 0.1150 \pm 0.0010 \, (exp) \pm 0.0013 \, (PDF) \pm 0.0015 \, (NP) \, ^{+0.0050}_{-0.0000} \, (scale)$. As shown in Fig. 3 (right), this value is in agreement with the world average value of $\alpha_s(M_Z) = 0.1181 \pm 0.0011$ derived in Ref. [10] as well as previous determinations obtained by the ATLAS and CMS collaborations [5, 11–15].

2.4 Azimuthal correlations

The two-final state partons, at leading order (LO) in pQCD, are produced back-to-back in the transverse plane and thus the azimuthal angular separation between the two highest p_T jets in the transverse plane, $\Delta\phi_{1,2} = |\phi_{jet1} - \phi_{jet2}|$, equals π. The production of a third or more high-p_T jets leads to a deviation from π in the azimuthal angle. The measurement of the azimuthal angular correlation (or decorrelation from π) in multijet topologies is proven to be an interesting tool to test theoretical predictions of multijet production processes. So measurements of the normalized inclusive 2-jet, 3-jet, and 4-jet cross sections differential in $\Delta\phi_{1,2}$ and of the normalized inclusive 3-jet, and 4-jet cross sections differential in $\Delta\phi_{2j}^{min}$ (minimum azimuthal angular separation between any two of the three or four leading p_T jets,) have been performed for several regions in the leading-jet transverse momentum p_T^{max} [21]. The measurements are performed using data collected during 2016 corresponding to an integrated luminosity of 35.9 fb^{-1} of proton-proton collisions at $\sqrt{s}$ = 13 TeV. The unfolded, normalized, inclusive 2-jet (left), 3-jet (middle), and 4-jet (right) cross section differential in $\Delta\phi_{1,2}$ is shown in Fig. 4 for the various p_T^{max} regions considered in the analysis. In the 2-jet case the $\Delta\phi_{1,2}$ distributions are strongly peaked at π and become steeper with increasing p_T^{max}. The $\Delta\phi_{1,2}$ distributions, in the 3-jet case become flatter at π since the dijet events are missing, and in the 4-jet case they become even more flat. The extension of $\Delta\phi_{1,2}$ correlations in inclusive 3-jet and 4-jet topologies are new results.
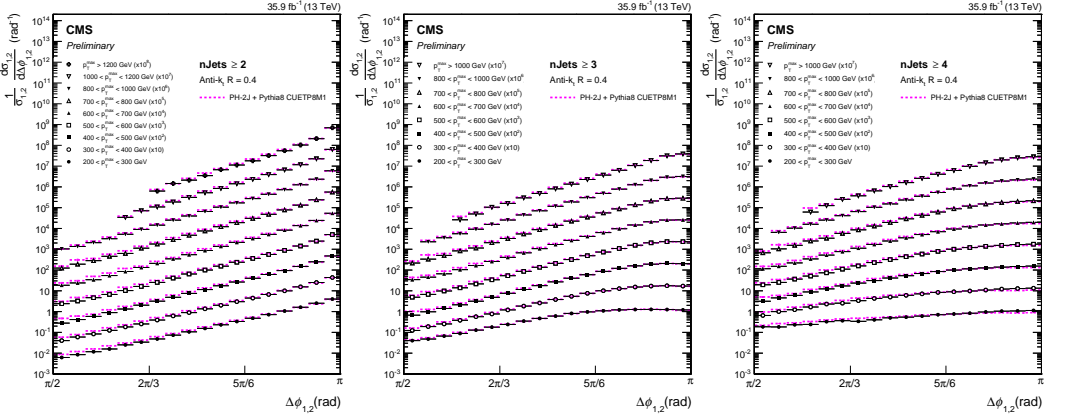

Figure 4. [21] Normalized inclusive 2-jet (left), 3-jet (middle) and 4-jet (right) cross section differential in $\Delta\phi_{1,2}$ for nine p_T^{max} regions, scaled by multiplicative factors for presentation purposes. Overlaid on the data are predictions from the PH-2J + PYTHIA8 event generator.

3 Jet charge and mass

At leading order (LO) in QCD, the type of partons that initiate jets can be distinguished and can be referred as quark jets, antiquark jets, or gluon jets. To distinguish signal from background, or to characterize a new particle, it is often important to identify the object initiating a jet by means of the properties of the reconstructed particles that define the jet. In particular, the electric charge quantum number of the original parton from which a jet is initiated can be estimated from a momentum-weighted sum of the charges of the particles in the jet. This observable is sensitive to the charge of the initiating quark or gluon and can provide constraints on models of jet formation. A study of

the jet charge distribution, unfolded for detector effects, with dijet events in pp collisions at $\sqrt{s} = 8$ TeV has been performed in various ranges of p_T [22]. This measurement is carried out for different definitions of jet charge as defined in equation 1, to gain a better understanding of the underlying models that can be used to improve the predictions of MC event generators. Figure 5 (left) compares data with the normalized charge distribution of the leading jet with $\kappa = 0.6$, initiated by either an up quark (u), down quark (d), or a gluon (g) in PYTHIA6. The charge distribution for jets initiated by quarks with positive electric charge peaks at positive values, with a mean of 0.166e, as opposed to that for jets initiated by negatively charged quarks, with a mean of -0.088e and gluons, with a mean of 0.013e, where e is the proton charge. This suggests that the jet charge can be used to differentiate statistically jets from quarks of different electric charge, or to distinguish jets initiated by a gluon or a quark.

$$Q^\kappa = \frac{1}{(p_T^{jet})^\kappa} \sum_i Q_i (p_T^i)^\kappa,$$

$$Q_L^\kappa = \sum_i Q_i \left(p_\parallel^i\right)^\kappa / \sum_i \left(p_\parallel^i\right)^\kappa,$$

$$Q_T^\kappa = \sum_i Q_i \left(p_\perp^i\right)^\kappa / \sum_i \left(p_\perp^i\right)^\kappa \tag{1}$$
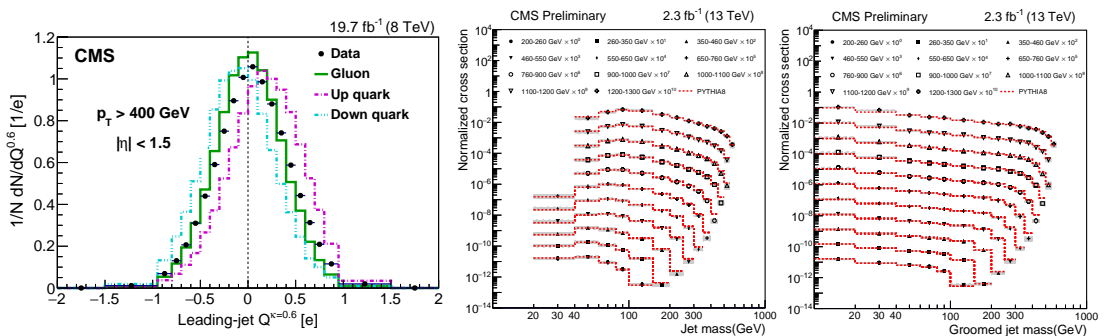

Figure 5. Comparison of jet charge distribution, Q^κ for leading jets and $\kappa = 0.6$, between data (points) and u, d, and g distributions from PYTHIA6 (left [22]). Results [23] of unfolding ungroomed (middle) and groomed (right) jets for all p_T bins. Bins with total uncertainty larger than 60% are not shown. The data are shown in markers for each p_T bin, scaled by a factor for better visibility. The predictions from PYTHIA8 are shown as a dashed red line.

Jet mass is more sensitive to the internal structure of jets, which is theoretically described by QCD parton showering. The recent techniques make use of the mass of the jets to investigate signals of physics beyond the standard model (BSM). The jet mass generated by QCD radiation is typically lower than the jet mass generated by hadronically-decaying heavy SM particles that have 2- and 3-prong decays such as W, Z, and H bosons, or top quarks. This can be exploited to identify BSM particles that decay into highly Lorentz-boosted SM particles ("boosted object"). CMS has performed a study [23] of double-differential jet cross section in bins of the ungroomed jet p_T in conjunction with the ungroomed and groomed jet mass using the 'soft drop" grooming algorithm [24], which is the same as the "mass drop" grooming algorithm for our choice of parameters. This observable is sensitive to the physics modeling, and could be used in future global fits for parameter tuning.

This analysis improves over previous results by using a more theoretically controlled jet grooming algorithm, as well as by unfolding in both p_T and mass. For ungroomed jets shown in Fig. 5 (middle), measurements from PYTHIA8 are found to predict the jet mass spectrum within uncertainties in the data for intermediate masses ($0.1 < m/p_T < 0.3$). For groomed jets as in Fig. 5 (right), the Sudakov peak is suppressed and the precision in the intermediate mass region ($0.1 < m/p_T < 0.3$) improves, since the grooming algorithm removes the portions of the jet arising from soft radiation.

4 Differential Z and W cross sections

Electroweak gauge boson production in pp collisions is an important probe of SM gauge boson inter-actions. The final states of W and Z decays have unique experimental signatures and the production cross sections for these processes are theoretically well understood and sensitive to deviations from the SM. The study of the cross sections and differential cross sections for a Z boson, decaying to dilepton channel, produced in association with jets in pp collisions at $\sqrt{s} = 8$ TeV [25] as well as at $\sqrt{s} = 13$ TeV [26] has been done. The cross sections are determined as functions of various rel-evant kinematic variables of jets. The predictions of a number of multileg generators with leading or next-to-leading order accuracy are compared with the measurements. The comparison shows the importance of including multiparton contributions in the matrix elements and the improvement in the predictions when next-to-leading order terms are included.

Similarly the differential cross sections have been measured for a W boson produced in associa-tion with jets in pp collisions at $\sqrt{s} = 8$ TeV [27] and at $\sqrt{s} = 13$ TeV [28]. The measured differential cross sections are compared with tree-level and higher-order recent event generators, as well as next-to-leading-order and next-to-next-to-leading-order theoretical predictions. The agreement of the gen-erators with the measurements builds confidence in their use for the simulation of W+jets background processes in searches for new physics at the LHC.

5 Heavy flavour jet physics

The associated production of vector bosons, W or Z, and jets originating from heavy-flavour quarks is a large background source in measurements of several SM processes, Higgs boson studies, and many searches for physics beyond the SM. The study of events with one or two well-identified and isolated leptons accompanied by heavy-flavour jets is crucial to refine the theoretical calculations in perturbative QCD, as well as to validate associated Monte Carlo techniques.

The cross section of the production of a Z boson associated with at least one jet originated by a c-quark in pp collisions at $\sqrt{s} = 8$ TeV corresponding to an integrated luminosity of 19.7 ± 0.5 fb^{-1}, is measured [29]. The cross sections ratio of the production of a Z boson and at least one c- or b-quark jet is also determined. The measured Z+c production cross section is σ (pp $\rightarrow$ Z + c + X) = 8.6 ± 0.5 (stat.) ± 0.7 (syst.) pb, and the cross sections ratio is σ (pp $\rightarrow$ Z + c + X)/σ (pp $\rightarrow$ Z + b + X) = 2.0 ± 0.2 (stat.) ± 0.2 (syst.). The measurements of Z+c production cross section and the cross sections ratio, inclusively and differentially as a function of p_T^{jet} are in agreement with the LO predictions from MADGRAPHand NLO predictions from MG5_AMC. Predictions from the MCFM program are lower than the measured Z+c cross section, both inclusive and differentially, as shown in 6 (left). A better description is reached in terms of the Z+c/Z+b cross sections ratio shown in 6 (right).

6 Top physics

The study of top production has a great discovery potential for physics beyond the standard model. It helps to test the production mechanisms, to check the validity of QCD, and to provide an important
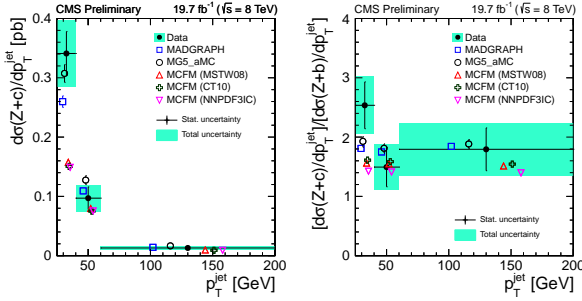
Figure 6. [29] Differential Z+c cross section (left) and Z+c/Z+b cross sections ratio (right) as a function of the transverse momentum of the jet. The solid rectangles indicate the total (statistical plus systematic) experimental uncertainty. Statistical and systematic uncertainties in the theoretical predictions are shown added in quadrature.

source of background in searches for physics beyond the standard model. Top quarks can decay leptonically t → Wb → (lν) (b-jet), and hadronically t → hadrons (three jets). In case of top pair production, di-leptonic decays of both quarks can be selected by requiring one electron and one muon of opposite charge, and at least two jets in the final state. The case when one decay is leptonic and the other one is hadronic is selected by asking for one electron or one muon, and at least four jets in the final state.

6.1 Differential $t\bar{t}$ production

Normalized double-differential cross sections for top quark pair ($t\bar{t}$) production are measured in pp collisions at $\sqrt{s}$ = 8 TeV corresponding to an integrated luminosity of 19.7 fb^{-1}[30]. The measurement is performed in the dilepton $e^{\pm}\mu^{\mp}$ final state. The $t\bar{t}$ cross section is determined as a function of various pairs of observables characterizing the kinematics of the top quark and $t\bar{t}$ system. The data is in agreement with calculations using pQCD at next-to-leading and approximate next-to-next-to-leading orders as well as with the fixed-order computations using MC Carlo event generators. The measured double-differential cross sections have been incorporated into a PDF fit, together with other data from HERA and the LHC. Including the $t\bar{t}$ data, there is a significant reduction in the uncertainties in the gluon distribution at large values of x and can be seen in Fig. 7 (left). The constraints provided by these data are competitive with those from inclusive jet data. This improvement exceeds that from using single-differential $t\bar{t}$ cross section data, thus strongly suggesting the use of the double-differential $t\bar{t}$ measurements in PDF fits.
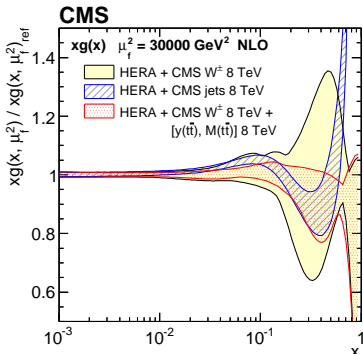

Figure 7. [30] The gluon distribution at μ^{2f} = 30000 GeV^2 , as obtained from the PDF fit to the HERA DIS data and CMS W$^{\pm}$ boson charge asymmetry measurements (shaded area), the CMS inclusive jet production cross sections (hatched area), and the W$^{\pm}$ boson charge asymmetry plus the double-differential $t\bar{t}$ cross section (dotted area).

6.2 t-channel single top quark production

The cross section of the t-channel single top quark production is measured using events with one muon and jets in the final state [31]. The cross section for the production of single top quarks and the ratio of the top quark to top antiquark production are measured together in a simultaneous fit where the results are used to evaluate the production cross section of single top antiquarks. Several kinematic variables are then combined into a multivariate discriminator to distinguish signal from background events. A fit to the distribution of the discriminating variable yields a total cross section of 238 ± 13 (stat) ± 29 (syst) pb and a ratio of top quark and top antiquark production of $R_{t-ch.} = 1.81 \pm 0.18$ (stat) ± 0.15 (syst).From the total cross section the absolute value of the CKM matrix element V_{tb} is calculated to be 1.05 ± 0.07 (exp) ± 0.02 (theo). All results are in agreement with the standard model predictions and previous measurements.

6.3 Top mass

The precise measurement of top quark mass (m_t), a fundamental parameter of the standard model (SM), can benefit the calculation of radiative corrections to several observables. The current m_t measurement methods exploit either the full kinematic reconstruction of top quark pair ($t\bar{t}$) events or alternative event topologies or observables that are sensitive to m_t variations. The latter can avoid intrinsic hadronization-related uncertainties and provide further understanding of the relation between the experimental results obtained for m_t and the mass parameters employed in theoretical calculations. The first measurement of the differential $t\bar{t}$ cross section has been performed in the ℓ + jets channel as a function of the leading-jet mass m_{jet} in the highly boosted top quark regime [32]. The measurement is carried out in a fiducial region with fully merged top quark decays in hadronic final states, corrected to the particle level. The predictions exceed the measurements of differential cross section as a function of the leading-jet mas as shown in Fig. 8 (left) whereas the normalized differential cross section shown in Fig. 8 (right) agrees with predictions from simulations, indicating the good quality of modelling the jet mass in highly boosted top quark decays. The normalized measurement is used to extract a value of m_t, in order to estimate the current sensitivity of the data. The value obtained is, $m_t = 170.8 \pm 9.0$ GeV which is consistent with the current LHC and Tevatron average of 173.34 ± 0.27 (stat) ± 0.71 (syst) GeV [33].
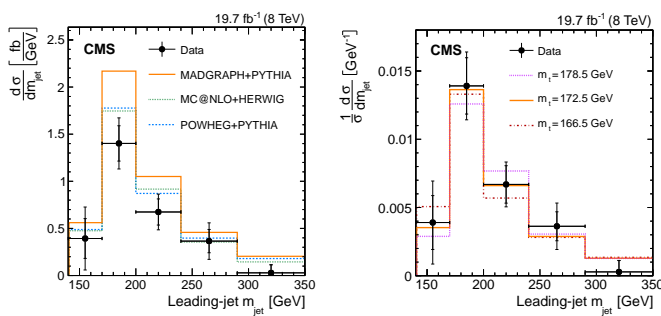

Figure 8. [32] Left : Measured particle-level differential $t\bar{t}$ cross sections as a function of the leading-jet mass, compared to predictions from MADGRAPH+PYTHIA, POWHEG+PYTHIA, and MC@NLO+HERWIG generators (lines). Right : The normalized particle-level $t\bar{t}$ differential cross section compared to predictions from MADGRAPH+PYTHIA for three values of m_t.

7 Summary

Jet production in proton-proton collisions is one of the main phenomenological predictions of perturbative Quantum Chromodynamics (pQCD). This paper summarizes the contribution of jets in the

measurements of characteristics of events, ranging from jet-charge to shapes as well as jet mass distributions. The measurements are compared to theoretical predictions including those matched to parton shower and hadronization. Along with this multi-differential jet cross-sections are presented over a wide range in transverse momenta from inclusive jets to multi-jet final states. These measurements have an impact on the determination of the strong coupling constant α_S as well as on parton density functions (PDFs). The electroweak boson production, whether inclusive or associated with charm or beauty quarks, gives insight into the flavour separation of the proton sea. Also the measurements of cross sections of jet and top-quark pair production are in particular sensitive to the gluon distribution in the proton and α_S.

References

[1] CMS Collaboration, JINST **3**, S08004 (2008).

[2] CMS Collaboration, JINST **12**, no. 10, P10003 (2017) arXiv:1706.04965 [physics.ins-det].

[3] M. Cacciari, G. P. Salam and G. Soyez, JHEP **0804**, 063 (2008) arXiv:0802.1189 [hep-ph].

[4] M. Cacciari, G. P. Salam and G. Soyez, Eur. Phys. J. C **72**, 1896 (2012) arXiv:1111.6097 [hep-ph].

[5] CMS Collaboration, JHEP **1703**, 156 (2017) arXiv:1609.05331 [hep-ex].

[6] CMS Collaboration, Eur. Phys. J. C **76**, no. 8, 451 (2016) arXiv:1605.04436 [hep-ex].

[7] CMS Collaboration, arXiv:1705.02628 [hep-ex].

[8] H1 and ZEUS Collaborations, Eur. Phys. J. C **75**, no. 12, 580 (2015) arXiv:1506.06042 [hep-ex].

[9] CMS Collaboration, CMS-PAS-SMP-16-008, http://cds.cern.ch/record/2253091

[10] Particle Data Group, Chin. Phys. C **40**, no. 10, 100001 (2016).

[11] CMS Collaboration, Eur. Phys. J. C **73**, no. 10, 2604 (2013) arXiv:1304.7498 [hep-ex].

[12] CMS Collaboration, Phys. Lett. B **728**, 496 (2014) arXiv:1307.1907 [hep-ex].

[13] CMS Collaboration, Eur. Phys. J. C **75**, no. 6, 288 (2015) arXiv:1410.6765 [hep-ex].

[14] CMS Collaboration, Eur. Phys. J. C **75**, no. 5, 186 (2015) arXiv:1412.1633 [hep-ex].

[15] ATLAS Collaboration, Phys. Lett. B **750**, 427 (2015) arXiv:1508.01579 [hep-ex].

[16] D0 Collaboration, Phys. Rev. D **80**, 111107 (2009) arXiv:0911.2710 [hep-ex].

[17] D0 Collaboration, Phys. Lett. B **718**, 56 (2012) arXiv:1207.4957 [hep-ex].

[18] H1 Collaboration, Eur. Phys. J. C **75**, no. 2, 65 (2015) arXiv:1406.4709 [hep-ex].

[19] H1 Collaboration, Eur. Phys. J. C **77**, no. 4, 215 (2017) arXiv:1611.03421 [hep-ex].

[20] ZEUS Collaboration, Nucl. Phys. B **864**, 1 (2012) arXiv:1205.6153 [hep-ex].

[21] CMS Collaboration, CMS-PAS-SMP-16-014, http://cds.cern.ch/record/2257685

[22] CMS Collaboration, JHEP **1710**, 131 (2017) arXiv:1706.05868 [hep-ex].

[23] CMS Collaboration, CMS-PAS-SMP-16-010, http://cds.cern.ch/record/2273393

[24] A. J. Larkoski *et al.*, JHEP **1405**, 146 (2014) arXiv:1402.2657 [hep-ph].

[25] CMS Collaboration, JHEP **1704**, 022 (2017) arXiv:1611.03844 [hep-ex].

[26] CMS Collaboration, CMS-PAS-SMP-15-010, http://cds.cern.ch/record/2114819

[27] CMS Collaboration, Phys. Rev. D **95**, 052002 (2017) arXiv:1610.04222 [hep-ex].

[28] CMS Collaboration, CMS-PAS-SMP-16-005, http://cds.cern.ch/record/2204927

[29] CMS Collaboration, CMS-PAS-SMP-15-009, http://cds.cern.ch/record/2202823

[30] CMS Collaboration, Eur. Phys. J. C **77**, no. 7, 459 (2017) arXiv:1703.01630 [hep-ex].

[31] CMS Collaboration, Phys. Lett. B **772**, 752 (2017) arXiv:1610.00678 [hep-ex].

[32] CMS Collaboration, Eur. Phys. J. C **77**, no. 7, 467 (2017) arXiv:1703.06330 [hep-ex].

[33] ATLAS and CDF and CMS and D0 Collaborations, arXiv:1403.4427 [hep-ex].